

Optical Photometry of Type II-P Supernova 2004dj in NGC 2403

Tianmeng Zhang¹, Xiaofeng Wang^{1,2}, Weidong Li³,
Xu Zhou¹, Jun Ma¹, Zhaoji Jiang¹, Jiansheng Chen¹

ABSTRACT

We present photometric data of the type II-P supernova (SN) 2004dj in NGC 2403. The multicolor light curves cover the SN from ~ 60 to 200 days after explosion, and are measured with a set of intermediate-band filters that have the advantage of tracing the strength variations of some spectral features. The light curves show a flat evolution in the middle of the plateau phase, then decline exponentially at the late times, with a rate of 0.10 ± 0.03 mag (10 days)⁻¹ in most of the filters. In the nebular phase, the spectral energy distribution (SED) of SN 2004dj shows a steady increase in the flux near 6600 Å and 8500 Å, which may correspond to the emission lines of H α and Ca II near-IR triplet, respectively. The photometric behavior suggests that SN 2004dj is a normal SN II-P. Compared with the light curves of another typical SN II-P 1999em, we estimate the explosion date to be June 10 ± 21 UT, 2004 (JD 2453167 \pm 21) for SN 2004dj. We also estimate the ejected nickel mass during the explosion to be $M(^{56}\text{Ni}) = 0.023 \pm 0.005 M_{\odot}$ from two different methods, which is typical for a SN II-P. We derive the explosion energy $E \approx 0.75_{-0.38}^{+0.56} \times 10^{51}$ erg, the ejecta mass $M \approx 10.0_{-5.2}^{+7.4} M_{\odot}$, and the initial radius $R \approx 282_{-122}^{+253} R_{\odot}$ for the presupernova star of SN 2004dj, which are consistent with other typical SNe II-P.

Subject headings: supernovae: general — supernovae: individual (SN 2004dj)—
techniques: photometric

¹National Astronomical Observatories of China, Chinese Academy of Sciences, Beijing 100012, P.R. China; ztm@vega.bac.pku.edu.cn, wxf@vega.bac.pku.edu.cn

²Physics Department and Tsinghua Center for Astrophysics, Tsinghua University, 100084, Beijing, China; wang_xf@mail.tsinghua.edu.cn

³Department of Astronomy, University of California, Berkeley, CA94720-34 11; weidong@astron.berkeley.edu

1. Introduction

Supernova (SN) 2004dj was discovered by K. Itagaki (Nakano et al. 2004) on 2004 July 31.76 (UT dates are used throughout this paper) in the nearby SBcd galaxy NGC 2403 at a distance of 3.3 ± 0.1 Mpc (Karachentsev et al. 2004). With a peak magnitude of 11.2 mag in the V band, SN 2004dj was the brightest supernova in the past decade. Spectroscopic observations of SN 2004dj show that it is a typical Type II Plateau SN (SN II-P), with prominent P-Cygni profiles in hydrogen Balmer lines (Patat et al. 2004). The main photometric characteristic of a SN II-P is that its light curve, unlike other SNe, does not decay rapidly after maximum, but shows a plateau phase for 60-100 days before decaying exponentially. The plateau phase originates from a balance between the receding photosphere in the expanding ejecta when the supernova is powered by the recombination of hydrogen previously ionized by the supernova shock. SNe II-P have long been thought to be produced by core-collapse of massive ($>8 M_{\odot}$) red supergiants that do not experience significant mass loss and retain most of their hydrogen-rich envelopes.

The optical position of SN 2004dj is measured to be R. A. = $07^{\text{h}}37^{\text{m}}17^{\text{s}}.04$, Dec = $+65^{\circ}35'57''.84$ (J2000.0; Nakano et al. (2004)). This is in good agreement with the *Chandra* X-ray position (Pooley & Lewin 2004) and the MERLIN radio position (Beswick et al. 2005). Using the astrometry of SN 2004dj, and also from geometrical registration between images of NGC 2403 before and after SN 2004dj occurred, both Maíz-Apellániz et al. (2004) and Wang et al. (2005) have convincingly shown that SN 2004dj occurred at a position coincident with Sandage Star 96 (hereafter S96) in the list of luminous stars and clusters in NGC 2403 published by Sandage (1984). Maíz-Apellániz et al. (2004) suggest that S96 is a young compact cluster with an age of 13.6 Myr and a total stellar mass of $\sim 24,000 M_{\odot}$, and estimate that the progenitor of SN 2004dj had a main-sequence mass of about $15 M_{\odot}$. Wang et al. (2005), on the other hand, suggest that S96 is an older (~ 20.0 Myr) and more massive ($\sim 96,000 M_{\odot}$) cluster, and that the progenitor of SN 2004dj may have a mass of $\sim 12 M_{\odot}$.

Studies of SN 2004dj itself may shed light on the nature of its progenitor, thus providing additional constraints on the properties of S96. In this paper, we present the results from our campaign of photometric followup of SN 2004dj from Aug 2004 to Jan 2005. The observations and data reduction are described in § 2, and the multicolor light curves and spectral energy distribution (SED) are presented in § 3. We estimate the explosion date, the reddening, the synthesized ^{56}Ni mass, and some explosion parameters for SN 2004dj in § 4. The conclusions are summarized in § 5.

2. Observations and Data Reduction

The observations of SN 2004dj were conducted with the 60/90 cm Schmidt telescope located at the Xinglong station of the National Astronomical Observatory of China (NAOC). A Ford Aerospace 2048×2048 CCD camera with a 15 micron pixel size is mounted at the Schmidt focus of the telescope. The field of view of the CCD is $58' \times 58'$ with a pixel scale of $1.7''$.

This telescope has a photometric system with 15 intermediate-band (FWHM \approx 200-400 Å) filters covering a wavelength range from 3000 Å to 10000 Å. Figure 1 shows the filters transmissions. These filters, also dubbed as the BATC system, were used to conduct a survey project among astronomers in Beijing, Arizona, Taipei, and Connecticut (Fan et al. 1996), and are designed to avoid contamination from the strongest and most variable night sky emission lines. The BATC magnitudes use the monochromatic AB magnitudes as defined by Oke & Gunn (1983). The standard stars HD 19445, HD 84937, BD+262606, and BD+174708 (Oke & Gunn 1983) are observed for flux calibration in the BATC observations. A full description of the BATC photometric system can be found elsewhere (Fan et al. 1996; Yan et al. 1999; Zhou et al. 2003).

We began to monitor SN 2004dj shortly after its discovery. The observations were obtained with 12 out of the 15 intermediate-band filters, and covered a period from 11 Aug 2004 to 10 Jan 2005. Typical exposure times are 300 s for each of the filters (longer for filters with the shortest wavelengths).

2.1. Photometry

As demonstrated by Maíz-Apellániz et al. (2004) and Wang et al. (2005), SN 2004dj occurred in a compact star cluster (S96) with $V \sim 18.0$ mag. The background of SN 2004dj is also contaminated by the spiral arms and nearby H II regions in NGC 2403. To perform proper photometry for SN 2004dj, subtraction of a template image of NGC 2403 without the SN is necessary. Usually observers have to wait for a long time until a SN fades enough to take the template image of its host galaxy, but fortunately for us, the host galaxy of SN 2004dj has been imaged as part of the Multicolor Sky Survey of BATC since 1995. The enormous archival images of NGC 2403 (Wang et al. 2005) provide us with the necessary template images for all the filters.

The goal of the image subtraction is to remove the contamination of the SN 2004dj flux by the compact cluster itself, and by the underlying emission from the spiral arms and nearby H II regions. To perform the subtraction, the observation with SN 2004dj is

first geometrically registered to the corresponding template image. The intensity of the two images are then matched by comparing the total fluxes of the stars in the images, and the point-spread-function (PSF) of the two images are convolved to the same level. Finally, the template is subtracted from the SN image, leaving a clean background for the SN. Figure 2 demonstrates this process.

The final step is to perform standard aperture photometry on the subtracted images. We used Pipeline II (a program developed to measure the magnitudes of point sources in BATC images) that is based on Stetson’s DAOPHOT package (Stetson 1987).

2.2. Calibration

A total of 45 photometric nights were used to calibrate 20 local standard stars in the field of SN 2004dj. For each photometric night, the afore-mentioned four standard stars were observed in a range of airmasses, and we derive iteratively the extinction curves and the slight variation of the extinction coefficients with time ($K + \Delta(UT)$) (Zhou et al. 2001). The instrumental magnitudes (m_{inst}) are transformed to the BATC AB magnitude (m_{batc}) (Zhou et al. 2001) by

$$m_{batc} = m_{inst} + [K + \Delta(UT)]\chi + C. \quad (1)$$

where χ is the airmass, and C is the zero point of magnitude.

Table 1 lists the final calibrated BATC magnitudes and their uncertainties of the 20 local standard stars. Figure 3 shows a $30' \times 30'$ image of the SN 2004dj field, together with the local standard stars within this frame.

These local standard stars are then used to transform the instrumental magnitudes of SN 2004dj to the BATC system, and the results are listed in Table 2. The estimated error shown in the parenthesis is a quadrature sum of the uncertainties in the bias and flat-field correction, the aperture photometry, and the calibrations. The main source of the error comes from the photometry, which is mainly caused by photon noises and the uncertainties in the image subtraction.

The last three columns of Table 2 list the broad-band Johnson-Cousins VRI magnitudes transformed from the BATC magnitudes. This transformation is done using the formula established by Zhou et al. (2003) which is given here as,

$$\begin{aligned} U &= b + 0.6801(a - b) - 0.8982 \pm 0.143, \\ B &= d + 0.2201(c - d) + 0.1278 \pm 0.076, \end{aligned}$$

$$\begin{aligned}
 V &= g + 0.3292(f - h) + 0.0476 \pm 0.027, \\
 R &= i + 0.1036 \pm 0.055, \\
 I &= o + 0.7190(n - p) - 0.2994 \pm 0.064.
 \end{aligned}
 \tag{2}$$

We need to point out, however, these transformation equations are derived from observations of Landolt standard stars, and may have relatively large uncertainties when applied to objects with broad lines, such as SNe.

3. Multicolor Light Curves

3.1. Light Curves of the first 200 days

The light curves of SN 2004dj in twelve intermediate-band filters (from d to p) are shown in Figure 4. Our photometry started at JD 2453230 and ended at JD 2453377, which corresponds to ~ 60 to 200 days after explosion if we adopt 2004 June 10 (JD 2453167) as the day of explosion for SN 2004dj (see the analysis in §4.1). Our observations show that SN 2004dj has a prominent plateau phase in all the passbands, suggesting that SN 2004dj is a SN II-P.

The light curves in all bands were characterized by a phase of 45 days of slowly decreasing luminosity (until JD 2453275). During this phase, the magnitude of SN 2004dj decreased by slightly different amount for different bands: 0.20 mag in n , 0.65 mag in d and g , and $\lesssim 0.5$ mag in the other bands.

After the plateau phase, the light curves show a rapid drop of ~ 2 mag in about 30 days, followed by a linear decay in magnitude that signals the onset of the nebular phase. The slow luminosity decline at the nebular phase, as listed in Table 3, is evident for SN 2004dj. The decline rates in most bands are 0.10 ± 0.03 mag (10 days) $^{-1}$ during the epochs from ~ 130 days to about 200 days after explosion. These late-time decay rates are in good agreement with the radioactive decay of ^{56}Co .

The evolution of the nebular-phase light curves in the i and n bands do not follow the other bands. Instead, the i -band flux remains almost constant, while the n -band flux increases slowly during the nebular phase. The peculiar behavior of the SN in these two bands may be due to the effect of strong emission lines, as discussed in the next section.

For comparison the light curves of SN 2004dj in the VRI band, transformed from our intermediate-band light curves using Eq.(2), are plotted along with the typical type II-P SN 1999em (Leonard et al. 2002; Hamuy et al. 2001) in Figure 5. Also plotted in the figure is the

V -band light curve of SN 2004dj as reported by Chugai et al. (2005). It can be seen that our transformed V -band magnitudes are consistent with those reported by Chugai et al. (2005) to within 0.1 mag, suggesting that our transformation to the broad-band V is reliable. This is consistent with expectations, since there are no strong emission or absorption lines at the V -band wavelength range for a typical SN II-P as demonstrated by Leonard et al. (2002). Compared to SN 1999em, SN 2004dj shows a similar evolution at the plateau phase, but a somewhat different evolution in the nebular phase, particularly in the R and I bands. While SN 1999em declines linearly in the R and I bands during the nebular phase, SN 2004dj is flat in the R band, and even brightens slightly in the I band. We emphasize, however, our transformed R and I magnitudes for SN 2004dj may bear large uncertainties due to the strong emission lines of $H\alpha$ and the Ca II IR triplet in our intermediate-band i and n , respectively. The different R and I evolution during the nebular phase for SN 1999em and SN 2004dj thus does not necessarily indicate a true difference between these two SNe.

3.2. The Spectral Energy Distribution (SED) Evolution

The spectral energy distribution (SED) of SN 2004dj can be best studied by spectroscopy such as these done by Korcakova et al. (2005). Alternatively, a rough SED can be constructed from the observed fluxes in various passbands at the same epoch. Because we have 12 intermediate-width passbands that cover 4000 Å to 10000 Å, we can study the SED evolution of SN 2004dj from our observations.

Because of the number of filters involved to observe SN 2004dj, it is not always possible to observe all bands in a single night, and our definition of the same epoch refers to a reference date ± 1 day. This is reasonable, considering the relatively slow evolution of SN 2004dj (except during the transition from the plateau to the nebular phase).

Figure 6 shows the SEDs of SN 2004dj at 61, 79, 112, 125, and 146 days after explosion. The SEDs are mostly a smooth function of the wavelength, except in the i and n bands, which are centered at 6700 Å and 8500 Å respectively. The deviation of these two bands from the smooth distribution of the other bands is likely to be caused by the strong lines in the spectrum of SN 2004dj. Because of the small heliocentric recession velocity (131 km s^{-1}) of NGC 2403, our i filter is centered at the $H\alpha$ emission, while the n filter covers the strong Ca II triplet $\lambda\lambda 8498, 8542, 8662$ line. From the well-studied SN II-P 1999em, Leonard et al. (2002) have shown that during the late part of the plateau phase, a SN II-P is dominated by strong lines with P-Cygni profiles. The emission component of $H\alpha$ is generally much stronger than the absorption, as a result, a net emission from $H\alpha$ when compared to the neighboring continuum is expected. In Figure 6, this is verified by the brighter magnitudes in the i band

than the h and j bands at 61 and 79 days after explosion. The absorption trough of the Ca II IR triplets, on the other hand, dominates the emission component at the same phase. This is verified by the relatively fainter magnitudes in the n band when compared to the m and o bands.

Leonard et al. (2002) also show that during the nebular phase (later than 120 days after explosion), the spectrum of SN 1999em is dominated by broad emissions. This is also true for the Ca II IR triplet, which shows multiple strong emission components but with little absorption. Our SEDs for SN 2004dj closely follow this trend: the n band flux changes from a relative absorption at 61 and 79 days after explosion, to a relative emission at 125 and 146 days after explosion. The smooth SED around n band at 112 days after explosion suggests that the absorption and emission components of the Ca II near-IR triplet is roughly balanced.

3.3. Color evolution

The $(V - R)$ (open circles) and $(V - I)$ (solid circles) color curves of SN 2004dj are shown in Figure 7, together with comparisons to those of SN 1999em (Leonard et al. 2002; Hamuy et al. 2001). Before ~ 120 day after explosion, the two SNe show similar color evolution [SN 2004dj has a slight bluer $(V - I)$ color]. In the nebular phase, however, there is a relatively big difference between the colors of the two SNe. SN 1999em remains nearly the same color, while SN 2004dj becomes progressively redder. Several factors may have contributed to this difference: there may be large uncertainties in our transformed R - and I -band magnitudes for SN 2004dj due to prominent emission lines of $H\alpha$ and Ca II near-IR triplet; the colors of SN 1999em may have large uncertainties as well, since the photometry was not performed after galaxy subtraction and background contamination may be significant due to the faintness of SN 1999em in the nebular phase.

Figure 7 also shows the evolution of SN 2004dj in two other colors: $(d - g)$ (solid squares) and $(j - n)$ (solid stars). The d and g bands, which are centered at $\sim 4540 \text{ \AA}$ and $\sim 5795 \text{ \AA}$, respectively, do not include strong lines of SNe II-P. The $(d - g)$ color thus roughly equals the $(B - V)$ color in the broad band. The $(B - V)$ color of SN 1999em and the $(d - g)$ color of SN 2004dj both evolve from blue to red after explosion, reach their reddest colors at ~ 130 -140 days, then become progressively bluer [at a rate of $\sim 0.50 \text{ mag (100 days)}^{-1}$] as the SNe enter the nebular phase. The $(d - g)$ color of SN 2004dj is bluer than the $(B - V)$ color of SN 1999em by $\sim 0.60 \pm 0.10 \text{ mag}$. This discrepancy may be caused by the systematic difference between the intermediate- and broad-band photometry. We were unable to convert our d -band photometry to B due to the lack of c -band (centered at $\sim 4220 \text{ \AA}$) observations

(cf. Eq. (2)).

The $(j - n)$ color of SN 2004dj shows a rapid and progressively redder evolution. The j band is centered at $\sim 7000 \text{ \AA}$ and roughly equals the broad R band. It does not include strong lines of a SN II-P. The n band is centered at $\sim 8500 \text{ \AA}$ and roughly equals the broad I band. This band, however, includes the strong Ca II IR triplet lines. Compared to the $(R - I)$ evolution of SN 1999em, the $(j - n)$ color of SN 2004dj evolves toward red at a much faster pace [$\sim 1.60 \text{ mag (100 days)}^{-1}$]. This is most likely caused by the brightening of the strong Ca II IR triplet emission in the n band of SN 2004dj.

4. Estimates of the explosion and the reddening

4.1. The explosion time

The spectra taken immediately after the discovery indicated that SN 2004dj was found long after the outburst (e.g., Patat et al. (2004), Korcakova et al. (2005)). This is also supported by the photometric observations. Our light curves of SN 2004dj (see Figure 4), obtained ~ 11 day after discovery, show that it was discovered in the middle of the plateau phase. Following the method of Hendry et al. (2005), we attempt to estimate the explosion time of SN 2004dj by comparing its light curve to those of other well-observed SNe II-P. This method adjusts the time and magnitude to find the best match using a χ^2 -minimizing technique. Assuming SN 2004dj evolves like SN 1999em, the comparison of the V -band data of the two SNe suggests an explosion date of $\text{JD } 2453168 \pm 1$ (June 11 ± 1 , 2004) for SN 2004dj, with a reduced χ^2 of 1.39. This estimate is consistent with that derived by Chugai et al. (2005) (JD 2453170) from a comparison between SN 2004dj and SN 1999gi. The uncertainty of our explosion date (± 1 day) comes from the statistical error of the fitting only.

The explosion date derived above assume SN 2004dj has the same duration of the plateau phase as SN 1999em. It was found from a sample of 13 SNe II-P, however, the average plateau duration varies by ± 21 days (Hamuy 2003; Hendry et al. 2005). As the error of the plateau phase duration is propagated directly to the error of the explosion date, we increase the uncertainty of our explosion date to ± 21 days. The final explosion date, $\text{JD } 2453168 \pm 21$, suggests that SN 2004dj was discovered at $\sim 50 \pm 21$ days after explosion.

4.2. The interstellar extinction

The Galactic extinction towards NGC 2403/SN 2004dj is known to be $A_V^{\text{gal}} = 0.13$ mag (Schlegel, Finkbeiner & Davis 1998), corresponding to a color excess of $E(B - V) = 0.04$ mag (adopting the standard reddening laws of Cardelli, Clayton & Mathis (1989)). However, it is rather difficult to accurately measure the extinction towards SN 2004dj within its host galaxy (NGC 2403).

With the assumption that all SNe II-P have the same intrinsic color at the end of the plateau phase (Eastman et al. 1996; Hamuy 2004), the color evolution of SN 2004dj may provide clues to its reddening. Since the early spectra of SN 2004dj are very similar to those of SN 1999em (Patat et al. 2004), it is reasonable to use SN 1999em as a comparison SN. We adopt a reddening of $E(B - V) = 0.10$ mag for SN 1999em following the analysis by Barbon et al. (2000) and Hamuy et al. (2001). A χ^2 -fitting algorithm was then used to compare the colors of SN 2004dj with those of SN 1999em from 60 days to 130 days after explosion. The $(V - R)$ fit yields a reddening of $E(B - V) \sim 0$ mag for SN 2004dj, which is less than the Galactic reddening of $E(B - V) = 0.04$ mag. The $(V - I)$ fit yields a negative reddening of $E(B - V) = -0.19 \pm 0.05$ mag for SN 2004dj (cf. Figure 6), which is physically unrealistic. Our failure to derive a reasonable reddening for SN 2004dj using the intrinsic color method suggests that the uncertainty of the method may be large, as also noted by Hamuy (2004). We also note that since our transformed R and I magnitudes for SN 2004dj are not reliable, the reddening estimates from the $(V - R)$ and $(V - I)$ color evolution are questionable as well.

An alternative way to determine the reddening towards SN 2004dj is to use the equivalent width (EW) of the Na I D interstellar absorption lines. The presence of narrow Na I D absorption lines in the early spectrum of SN 2004dj, with $\text{EW} \sim 1.1 \text{ \AA}$, was reported by Patat et al. (2004). Based on this EW, Patat et al. (2004) estimated the reddening towards SN 2004dj within NGC 2403 is $E(B - V) = 0.18$ mag. The correlation between the EW of the Na I D interstellar absorption and the reddening, unfortunately, is quite uncertain. Using $\text{EW} = 1.1 \text{ \AA}$ and the prescription by Barbon et al. (1990), we derived a reddening of $E(B - V) = 0.28$ mag for SN 2004dj within NGC 2403. The prescription by Munari & Zwitter (1997), on the other hand, suggests a host galaxy reddening of $E(B - V) = 0.40$ mag. The average of the three measurements is $E(B - V) = 0.29 \pm 0.11$ mag. When combined with the Galactic component, the total reddening towards SN 2004dj is $E(B - V) = 0.33 \pm 0.11$ mag, which is consistent with the estimate $E(B - V) = 0.35 \pm 0.05$ mag from the spectral fit to the SED of S96 (Wang et al. 2005).

We adopt $E(B - V) = 0.33 \pm 0.11$ mag ($A_V = 1.02 \pm 0.34$ mag) as our final reddening estimate for SN 2004dj. When this correction for reddening is applied, we obtain the intrinsic

peak brightness for SN 2004dj as $M_{max}^V = -16.70 \pm 0.35$ mag (the major error is contributed from the uncertainty of the reddening correction), which is typical for a SN II-P.

5. The bolometric light curve and the mass of ^{56}Ni

5.1. The bolometric light curve

SNe II-P produce a large range of ^{56}Ni masses from $\sim 10^{-3}$ to $> 10^{-1}M_{\odot}$. Hamuy (2003) showed that a correlation exists between the amount of ^{56}Ni produced in the explosion and the absolute magnitude in the V -band during the plateau phase. Our observations suggest that SN 2004dj has a plateau luminosity of $M_p^V = -16.55 \pm 0.35$ mag. We therefore estimate that amount of ^{56}Ni produced during the SN 2004dj explosion to be intermediate between $0.01M_{\odot}$ and $0.1M_{\odot}$ if it follows the correlation shown in Figure 3 of Hamuy (2003). To better estimate the mass of ^{56}Ni produced during the explosion, we construct the “bolometric” light curve for SN 2004dj by integrating the flux in the 12 intermediate bands. The decline rate of the “bolometric” light curve for SN 2004dj is smaller than that of SN 1987A [0.73 ± 0.30 mag (100 days) $^{-1}$ vs. 1.06 ± 0.06 mag (100 days) $^{-1}$]. This pseudo-bolometric light curve may not be accurate due to our lack of the ultraviolet and infrared photometry for SN 2004dj. The resulting light curve, together with that of SN 1987A (Suntzeff & Bouchet 1990), are shown in Figure 8.

5.2. The ejected ^{56}Ni mass

5.2.1. The ^{56}Ni mass from the bolometric light curve

The luminosity of a SN II-P during the nebular exponential decay is controlled by the radioactive decay of the newly synthesized materials during the SN explosion (Weaver & Woosley 1980). If all the gamma rays generated by the $^{56}\text{Co} \rightarrow ^{56}\text{Fe}$ decay are fully thermalized, the decline rate of the light curve at the nebular phase should equal the ^{56}Co decay slope, and the mass of ^{56}Ni can be determined from the bolometric luminosity on the exponential tail in Figure 8 using the equation below (Hamuy 2003),

$$M_{\text{Ni}} = 7.866 \times 10^{-44} L \exp\left[\frac{(t - t_0)/(1 + z) - \tau_{\text{Ni}}}{\tau_{\text{Co}}}\right] M_{\odot}, \quad (3)$$

where t_0 is the explosion epoch, $\tau_{\text{Ni}} = 6.1$ days is the half-life of ^{56}Ni and $\tau_{\text{Co}} = 111.26$ days is e -folding time of ^{56}Co . L is the tail luminosity which is calculated by Eq.(1) of Hamuy (2003).

Using Eq.(3) we estimated M_{Ni} from each point on the late-time tail for SN 2004dj. The average of these mass estimates is $M_{\text{Ni}} = 0.025 \pm 0.010 M_{\odot}$, which is similar to that produced in SN 1999em ($M_{\text{Ni}} = 0.021 \pm 0.002 M_{\odot}$; Elmhamdi et al. (2003b)). The error in the ^{56}Ni mass is caused by the uncertainties in the explosion date, extinction, and the distance to NGC 2403.

5.2.2. The ^{56}Ni Mass from the “Steepness of Decline” Correlation

A correlation between the maximum gradient at the transition phase in the V band and the photometric estimate of $M(^{56}\text{Ni})$ has been reported by Elmhamdi et al. (2003a). A characteristic steepness parameter has been defined as $S = -dM_V/dt$, which corresponds to the maximum gradient rate of the light curve between plateau and nebular phase. Based on a sample of ten SNe II-P, they derived a linear relation between M_{Ni} (in unit of solar mass M_{\odot}) and S ,

$$\log M(^{56}\text{Ni}) = -6.2295 S - 0.8147. \quad (4)$$

Using the template flux from Eq.(1) of Elmhamdi et al. (2003a), we fit the light curves of SN 2004dj in several intermediate bands (f , h , j , k and m) that do not include strong emission or absorption lines, as well as in the transformed V band. The results are shown in Figure 9. For each band, the upper panel shows the best fit for the light curve, while the lower panel shows the profiles of S and the derived inflection time t_u . The average value of the “steepness” parameter S from fitting the light curves is 0.141 ± 0.005 , which suggests a ^{56}Ni mass of $0.020 \pm 0.002 M_{\odot}$. This value is consistent with that determined from the bolometric light curve study, providing support for the validity of the steepness parameter method. However, one should note that in the case of SN 2003gd, Hendry et al. (2005) find the mass of ^{56}Ni estimated from this method is significantly lower than that from tail luminosity method.

The above two determinations allow us to estimate the amount of ^{56}Ni mass in SN 2004dj is $0.023 \pm 0.005 M_{\odot}$. This value is typical for a normal SN II-P, and is consistent with the independent estimates from the $\text{H}\alpha$ luminosity or comparison with SN 1987A (Chugai et al. 2005).

6. The progenitor star of SN 2004dj

The detailed photometric observations may provide valuable constraints on the explosion parameters of the supernova and hence on the progenitor star (Hendry et al. 2005). The hydrodynamical models of SNe II-P light curves originally proposed by (Litvinova & Nadyozhin 1985) predicted a correlation between the phenomenological parameters (the plateau duration, the absolute magnitudes and photosphere velocity at the middle of the plateau) and the physical parameters such as the explosion energy E_{exp} , the ejecta mass M_{ej} , and the initial radius of the pre-supernova star R_{pSN} .

Although the early observations immediately after the explosion were unavailable for SN 2004dj, the fact that it resembles SN 1999em allows us to make an assumption about the length of its plateau phase ($\Delta t \sim 80 \pm 21$ days). Adopting the reddening estimate in § 4.2 and standard reddening law of $R_V = 3.1$, we derived the absolute magnitude during the plateau phase as $M_V = -16.55 \pm 0.35$ mag. From the spectrum observed at 52 days after explosion (Patat et al. 2004), we estimate a photosphere velocity ($v_{ph} \approx 3933 \pm 189$ km s⁻¹) from weak Fe II absorption lines near 5000 Å. With these observed parameters, we can estimate the explosion parameters by using the simple approximation formulae from (Litvinova & Nadyozhin 1985), which are here give as

$$\log\left(\frac{E_{exp}}{10^{51}erg}\right) = 0.135 M_V + 2.34 \log\left(\frac{\Delta t}{days}\right) + 3.13 \log\left(\frac{v_{ph}}{10^3 km s^{-1}}\right) - 4.205, \quad (5)$$

$$\log\left(\frac{M_{ej}}{M_\odot}\right) = 0.234 M_V + 2.91 \log\left(\frac{\Delta t}{days}\right) + 1.96 \log\left(\frac{v_{ph}}{10^3 km s^{-1}}\right) - 1.829, \quad (6)$$

$$\log\left(\frac{R_{pSN}}{R_\odot}\right) = -0.572 M_V - 1.07 \log\left(\frac{\Delta t}{days}\right) - 2.74 \log\left(\frac{v_{ph}}{10^3 km s^{-1}}\right) - 3.350. \quad (7)$$

Combing the observed parameters and the above relations yields an explosion energy $E_{exp} \approx 0.75_{-0.38}^{+0.56} \times 10^{51}$ erg, an ejecta mass $M_{ej} \approx 10.0_{-5.2}^{+7.4} M_\odot$, and an initial radius $R_{pSN} \approx 282_{-122}^{+253} R_\odot$ for the pre-supernova star of SN 2004dj. Taking into account approximately 2–3 M_\odot for the remnant neutron star and the mass loss lost by stellar wind prior to the SN explosion, we obtain a possible range of 8–20 M_\odot for the main sequence mass of the progenitor, which is consistent with the estimates determined by the turnoff mass of the star cluster hosting SN 2004dj (Wang et al. 2005; Maíz-Apellániz et al. 2004). The derived parameters for the progenitor of SN 2004dj suggest it was a K0–M0 supergiant (Cox 2000).

7. Conclusions

This paper presents the photometry of SN 2004dj taken with 12 intermediate-band filters, and obtained from ~ 60 to 200 days after the explosion. Our observations show that SN 2004dj was discovered in the middle of the plateau phase. The multicolor light curves show a plateau phase of about 45 days, a transition period of about 30 days during which the SN declines dramatically, and a nebular phase during which the SN declines at a rate of $\sim 0.10 \pm 0.03 \text{ mag (10 days)}^{-1}$ (consistent with the decay rate of ^{56}Co).

The SEDs for SN 2004dj are constructed from the measured flux in the 12 passbands. These SEDs show an evolution that is similar to the spectral evolution of a normal SN II-P. A flux peak near 6600 \AA is observed, which is consistent with the strong $\text{H}\alpha$ emission seen in these objects. The flux around 8500 \AA evolves from a flux deficit to a flux peak, consistent with the evolution of the strong Ca II near-IR triplet line.

By comparing the light curve of SN 2004dj to the well observed SN II-P 1999em, we estimate the explosion date for SN 2004dj to be $\text{JD } 2453168 \pm 21$ (June 11, 2004), approximately 50 day before the actual discovery of SN 2004dj.

Finally, we estimate the ^{56}Ni mass synthesized during the SN 2004dj explosion using two methods: the bolometric tail luminosity and the “steepness” parameter. These methods yield a value of $M_{\text{Ni}} = 0.023 \pm 0.005 M_{\odot}$ for SN 2004dj, which is typical for a normal SN II-P. Comparing our observed parameters of SN 2004dj with the analytical models of SN II-P light curves (Litvinova & Nadyozhin 1985), We derive for SN 2004dj an explosion energy of $0.75_{-0.38}^{+0.56} \times 10^{51} \text{ erg}$, an ejecta mass of $10.0_{-5.2}^{+7.4} M_{\odot}$, and an initial radius of $282_{-122}^{+253} R_{\odot}$. These parameters suggest that the progenitor of SN 2004dj is likely to be a K0–M0 type supergiant.

This work was supported by National Science Foundation of China (NSFC grant 10303002, 10473012 and 10573012), National Key Basic Research Science Foundation (NKBRFSF TG199075402), and basic Research Foundation at Tsinghua University (2005). The work of W.L. at U.C. Berkeley is supported by National Science Foundation grant AST-0307894. We thank Dr. Yang Yanbin for his helpful discussions on the reduction of the photometric data.

REFERENCES

- Barbon, R., Benetti S., Rosino L., Cappellaro E., Turatto, M. 1990, *A&A*, 237, 79
- Barbon, R., Carraro, G., Munari, U., Zwitter, T., & Tomasella, L. 2000, *A&AS*, 144, 451
- Beswick, R. J., Muxlow, T. W. B., Argo, M. K., Pedlar, A., Marcaide, J. M., & Wills, K. A. 2005, *ApJ*, 623, L21
- Cardelli, J. A., Clayton, G. C., & Mathis, J. S. 1989, *ApJ*, 345, 245
- Chugai, N. N., et al. 2005([astro-ph/0507689](#))
- Cox A. N. 2000, in *Allen’s Astrophysical Quantities*. Fourth edition
- Eastman, R. G., Schmidt, B. P., & Kirshner, R. P. 1996, *ApJ*, 466, 911
- Elmhamdi, A., et al. 2003, *MNRAS*, 338, 939
- Elmhamdi, A., Chugai, N. N., & Danziger, I. J. 2003, *A&A*, 404, 1077
- Fan, X., et al. 1996, *AJ*, 112, 628
- Hamuy, M., et al. 2001, *ApJ*, 558, 615
- Hamuy, M. 2003, *ApJ*, 582, 905
- Hamuy, M. 2004, in *Measuring and Modeling the Universe, from the Carnegie Observatories Centennial Symposia*. Carnegie Observatories Astrophysics Series. Edited by W. L. Freedman, 2004. Pasadena: Carnegie Observatories, *The Latest Version of the Standardized Candle Method for Type II Supernovae*, [astro-ph/0301281](#)
- Hendry, M. A., et al. 2005, *MNRAS*, 359, 906
- Karachentsev, I. D., Karachentseva, V. E., Huchtmeier, W. K., & Makarov, D. I. 2004, *AJ*, 127, 2031
- Korcakova, D., et al. 2005, *Information Bulletin on Variable Stars*, 5605, 1
- Leonard, D. C., Filippenko, A. V., Li, W., et al., 2002, *AJ*, 124, 2490
- Litvinova, I. Yu., & Nadyozhin D. K. 1985, *Sov. Astron. Lett.*, 11, 145
- Maíz-Apellániz, J. et al. 2004, *ApJ*, 615, L113
- Munari, U., & Zwitter, T. 1997, *A&A*, 318, 269

- Nakano, S., Itagaki, K., Bouma, R. J., Lehky, M. & Hornoch, K. 2004, IAUC, 8377
- Oke, J. B., & Gunn, J. E. 1983, ApJ, 266, 713
- Patat, F., Benetti, S., Pastorello, A., Filippenko, A. V. & Aceituno, J. 2004, IAUC, 8378
- Pooley, D., & Lewin, W. H. G. 2004, IAUC, 8390
- Sandage, A. 1984, AJ, 89, 630
- Schlegel D. J., Finkbeiner D. P., & Davis M. 1998, ApJ, 500, 525
- Stetson, P. B. 1987, PASP, 99, 191
- Suntzeff, N. B., & Bouchet, P. 1990, AJ, 99, 650S
- Wang, X. F., et al. 2005, ApJ, 626, L89
- Weaver, T. A., & Woosley, S. E., 1980, Ann. N. Y. Acad. Sci, 336, 335
- Weis, K., Bomans, D. J., Klose, S., & Spiller, F, 2004, IAUC, 8384
- Yan, H. et al. 2000, PASP, 112, 691
- Zhou, X. et al. 2001, ChJAA, 1, 372
- Zhou, X. et al. 2003, A&A, 397, 361

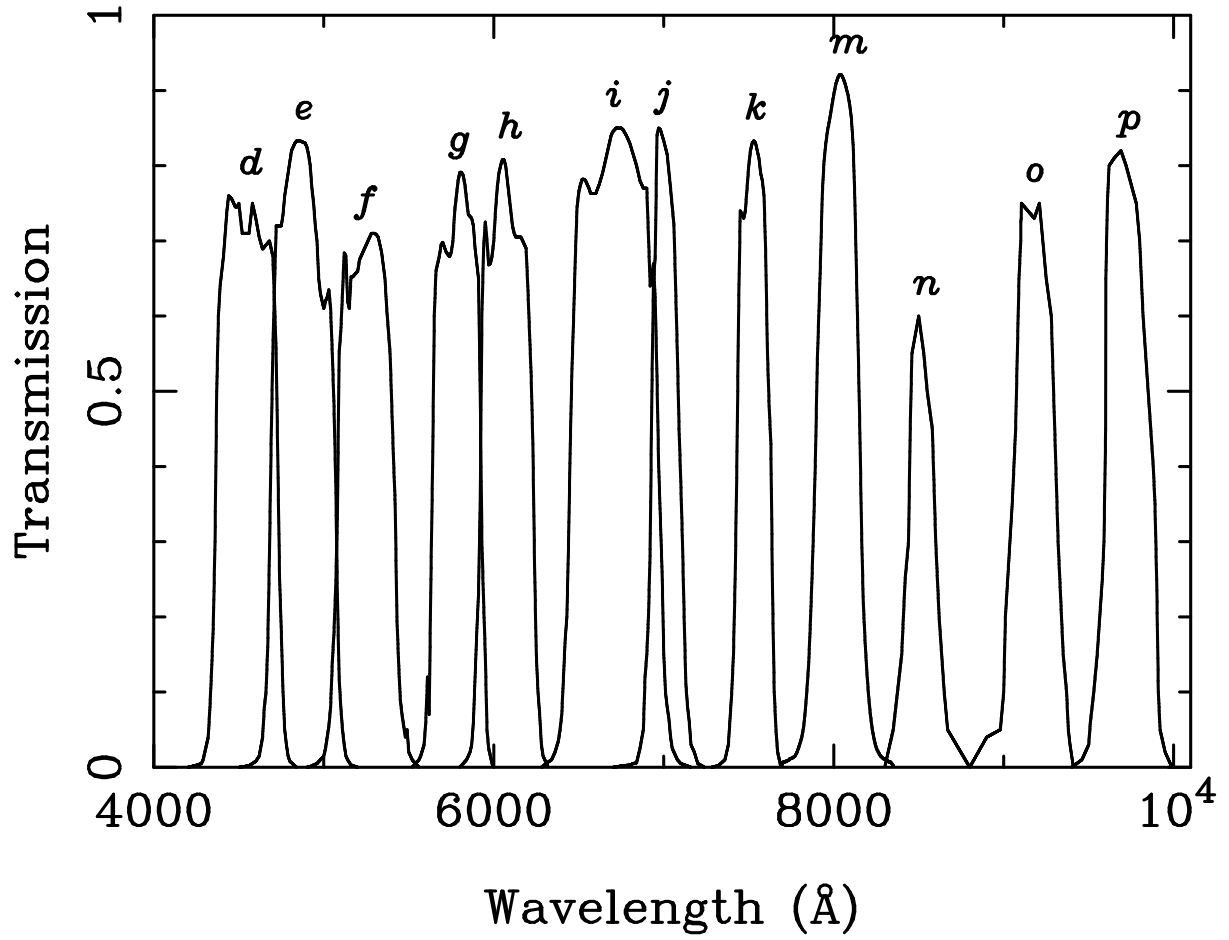


Fig. 1.— The transmission curves of the 12 bands (*d* – *p*) in the BATC system.

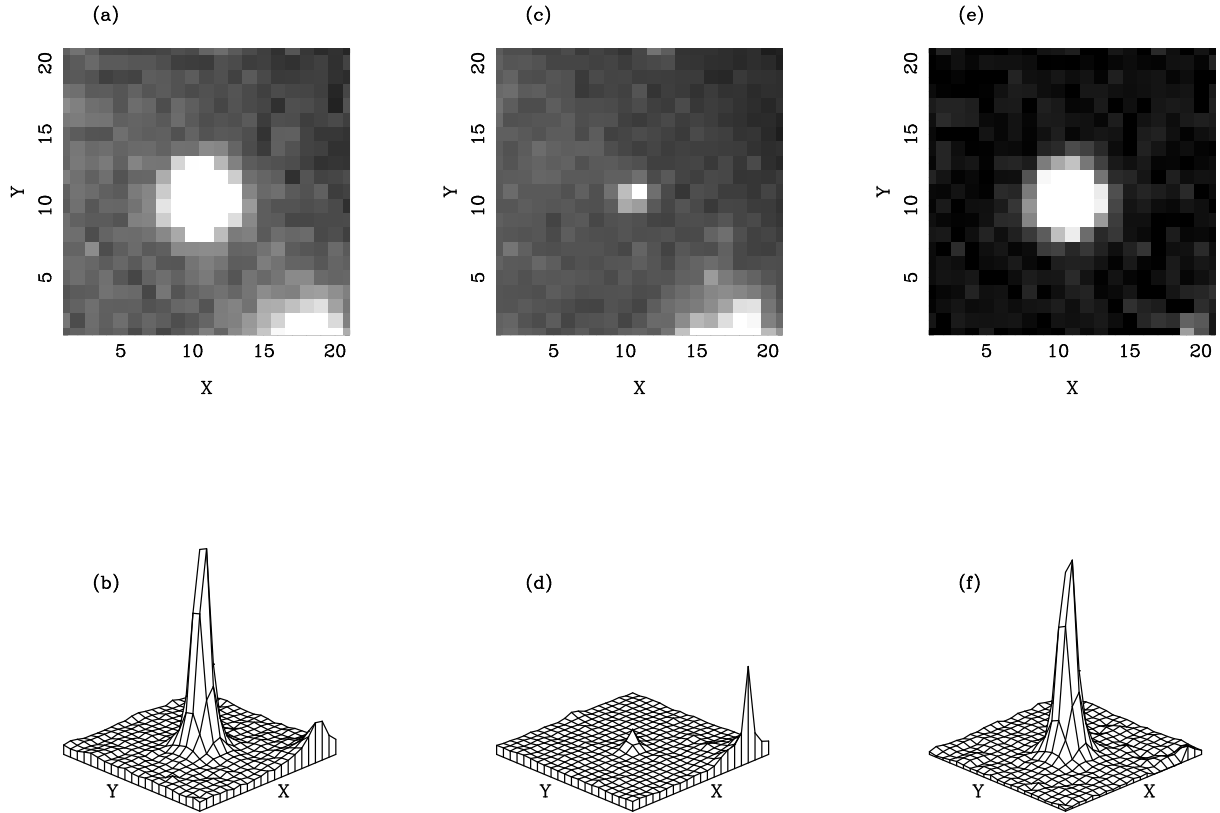


Fig. 2.— Demonstration of the image subtraction process. (a) The original image of SN 2004dj; (b) The surface plot for the original image; (c) The template image before SN 2004dj; (d) The surface plot for the template image; (e) The image of SN 2004dj after galaxy subtracting, notice the nearby H II region is cleanly subtracted; (f) the surface plot for the subtracted image.

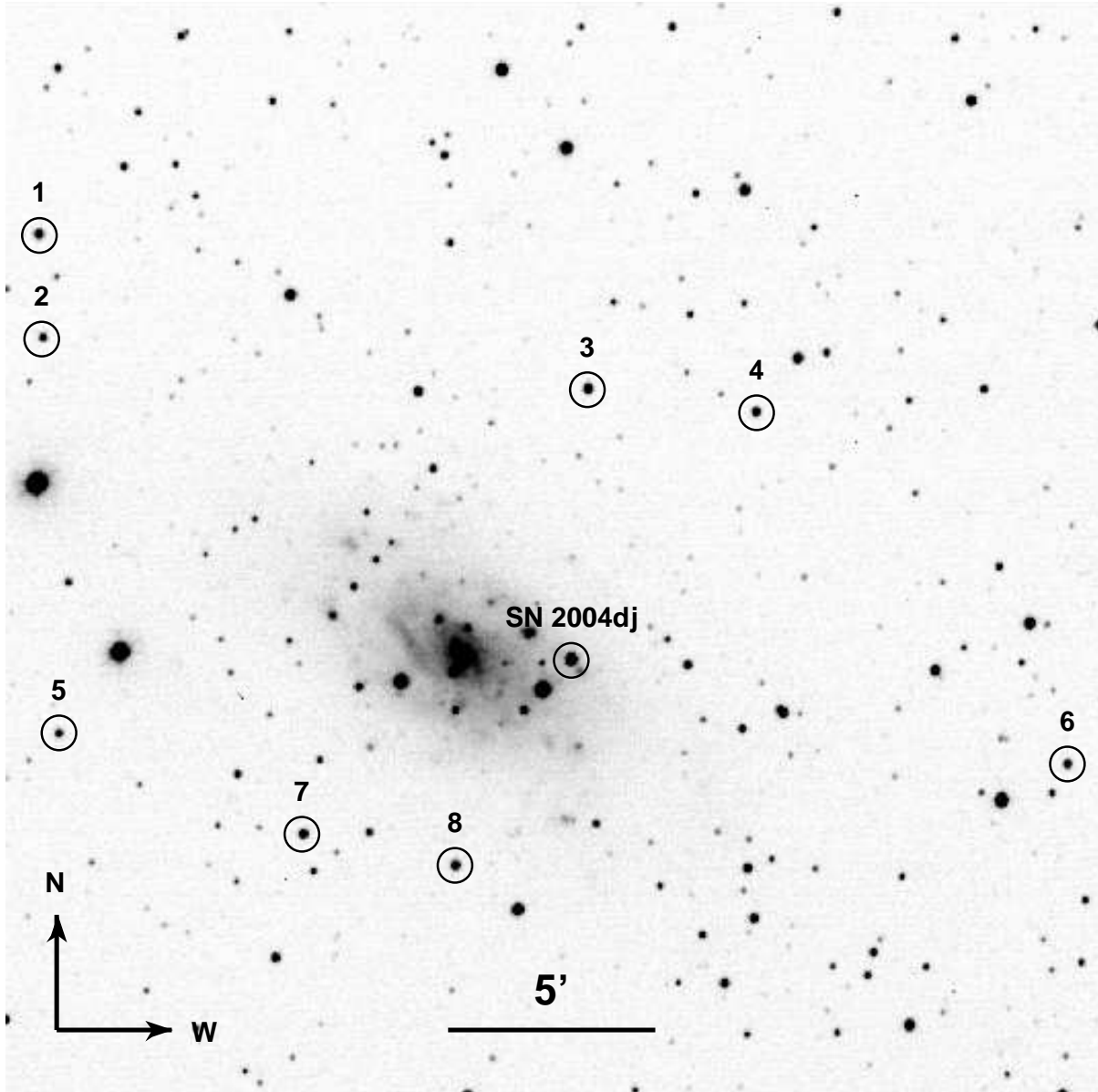


Fig. 3.— SN 2004dj in NGC 2403. This is an *i*-band image taken with the BATC 60/90 cm Schmidt telescope on 2004 August 12 UT, 13 days after discovery. The SN and some reference stars are marked.

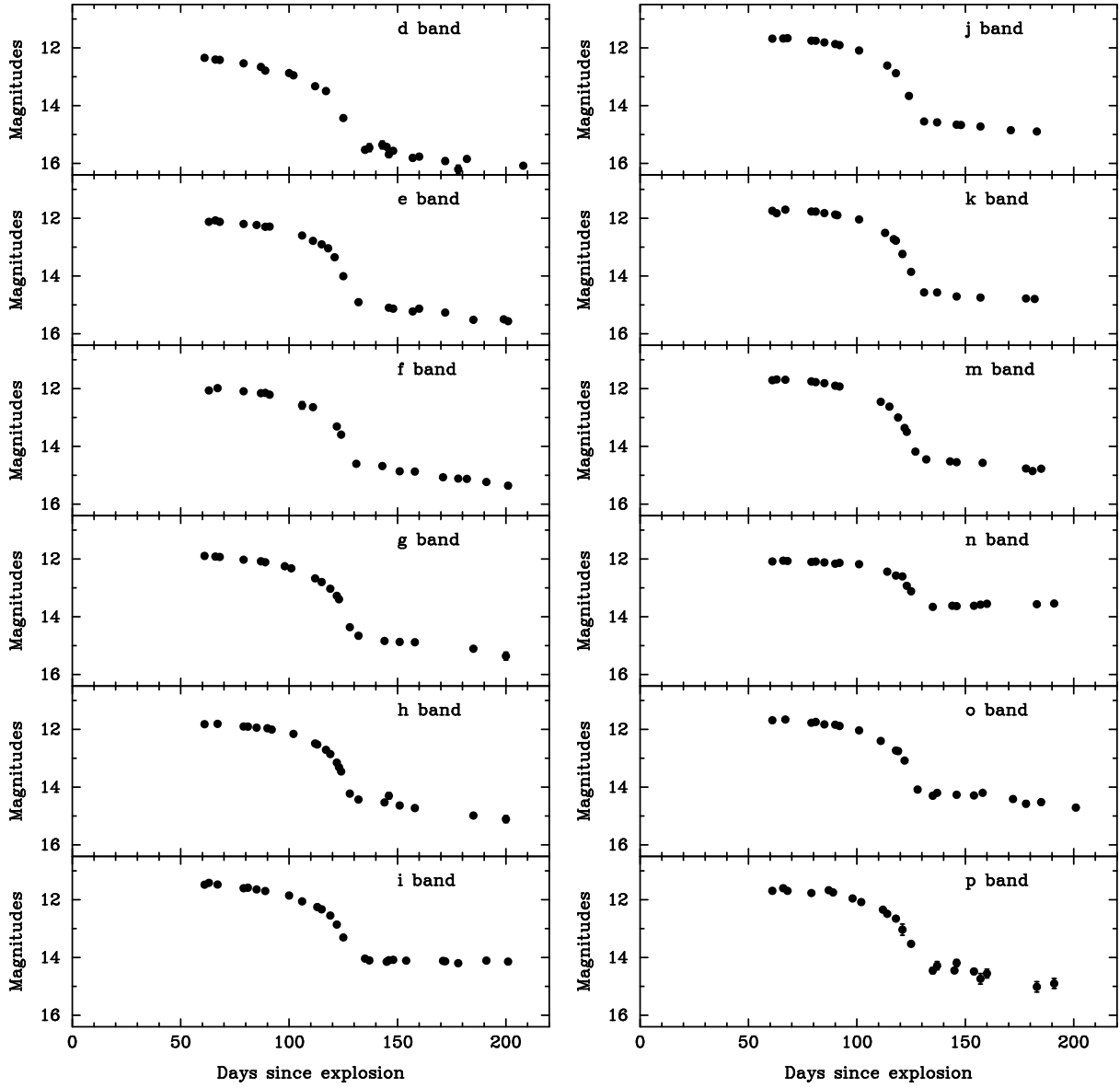


Fig. 4.— Light curves of SN 2004dj in the 12 intermediate bands.

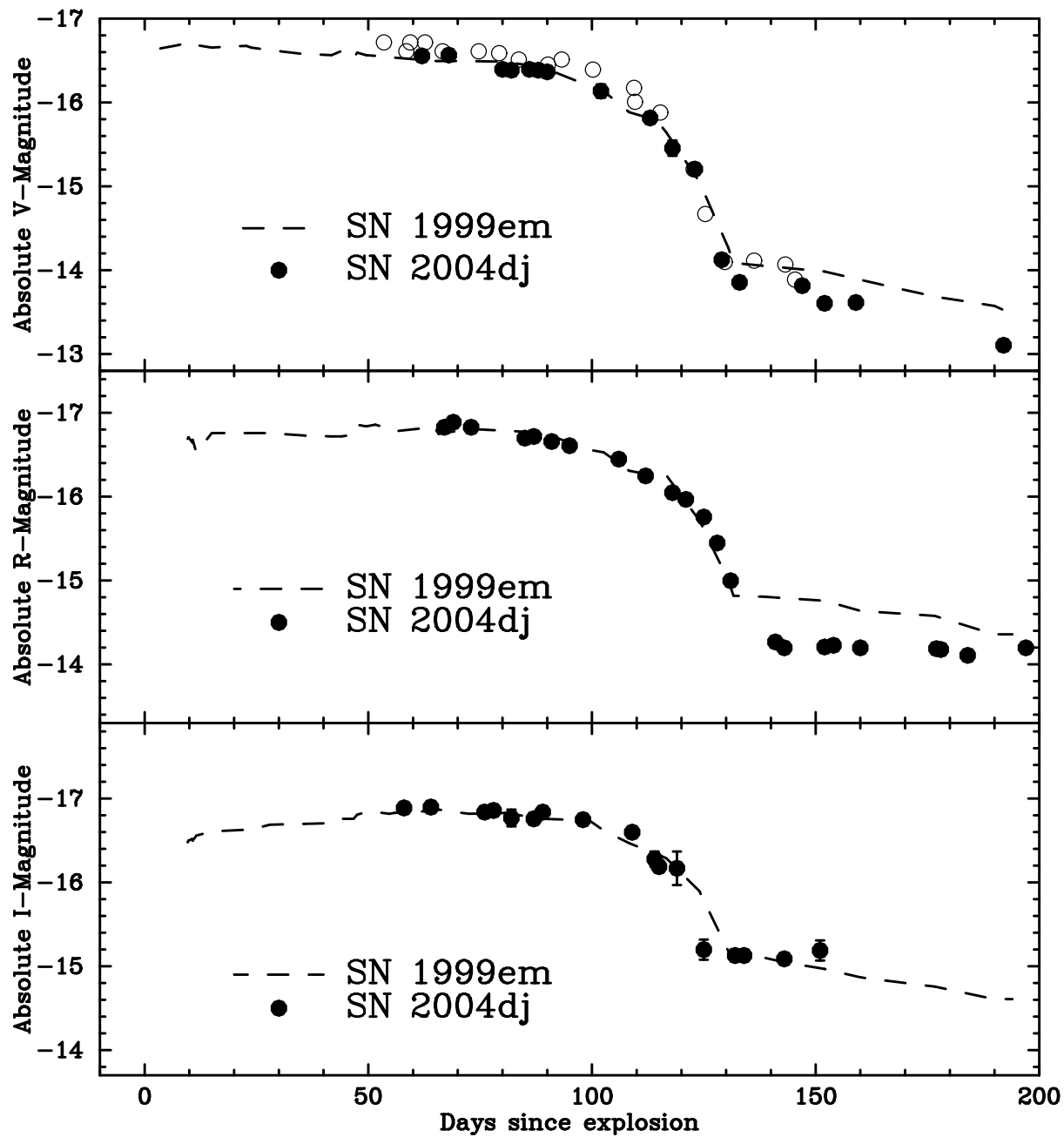


Fig. 5.— Broad-band *VRI* light curves of SN 2004dj (filled symbols). Also over-plotted are light curve of SN 1999em from Hamuy et al. (2001) and Leonard et al. (2002). The *V*-band magnitudes reported by Chugai et al. (2005) are shown as open symbols.

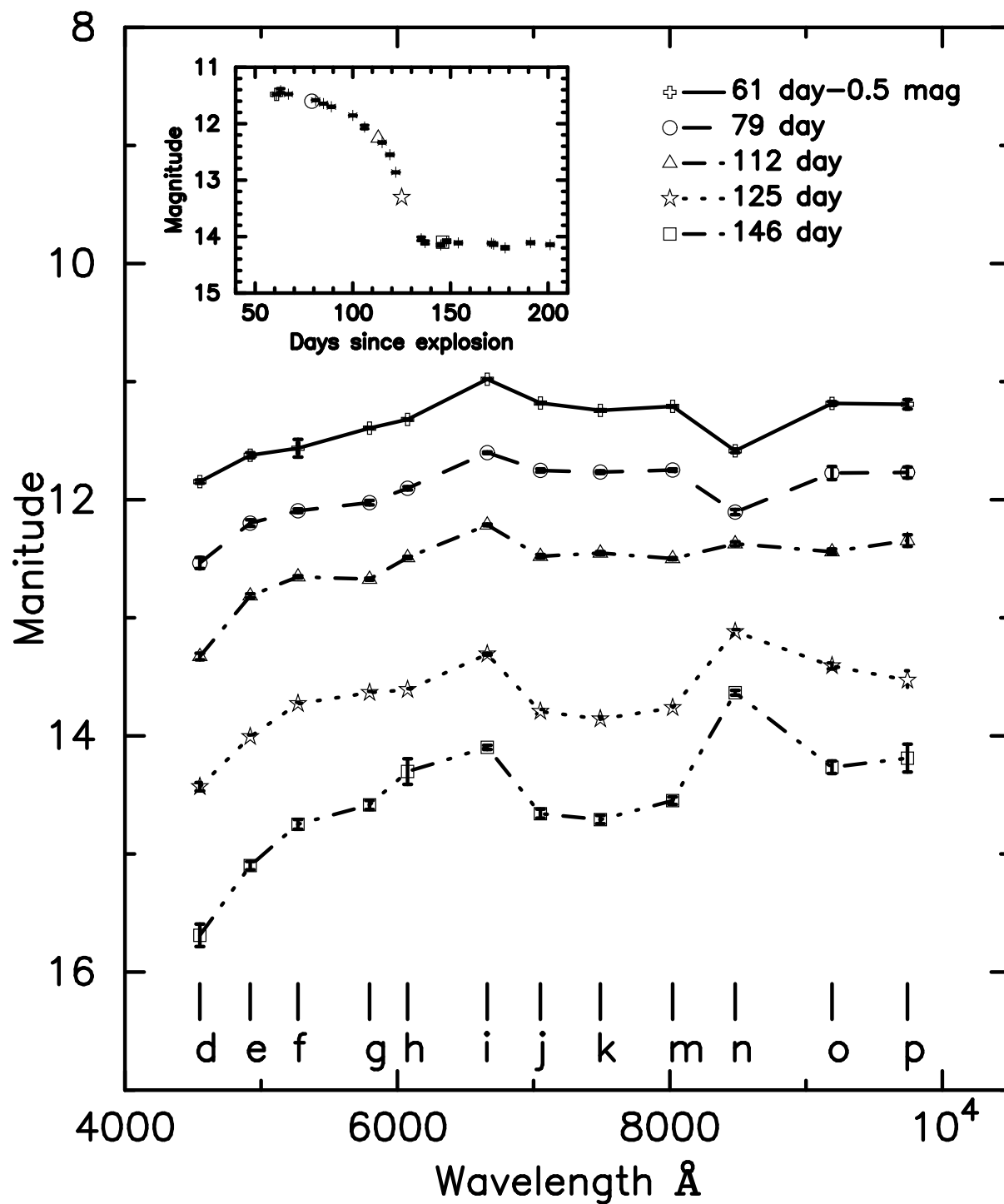


Fig. 6.— The spectral energy distribution (SED) of SN 2004dj at days 61, 79, 112, 125, and 146 after explosion. The inset shows the location of these SEDs in the *i*-band light curve.

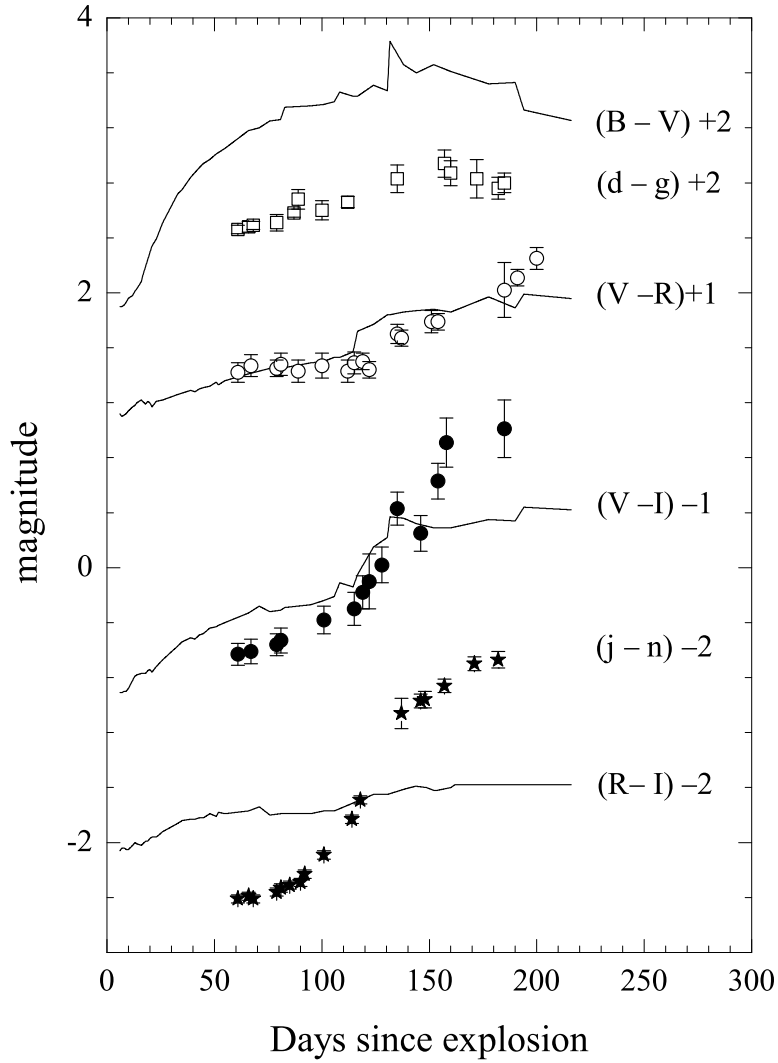


Fig. 7.— The color curves of SN 2004dj which have been arbitrarily shifted in magnitudes for clarity. The solid lines represent the data of SN 1999em from Hamuy et al. (2001) and Leonard et al. (2002).

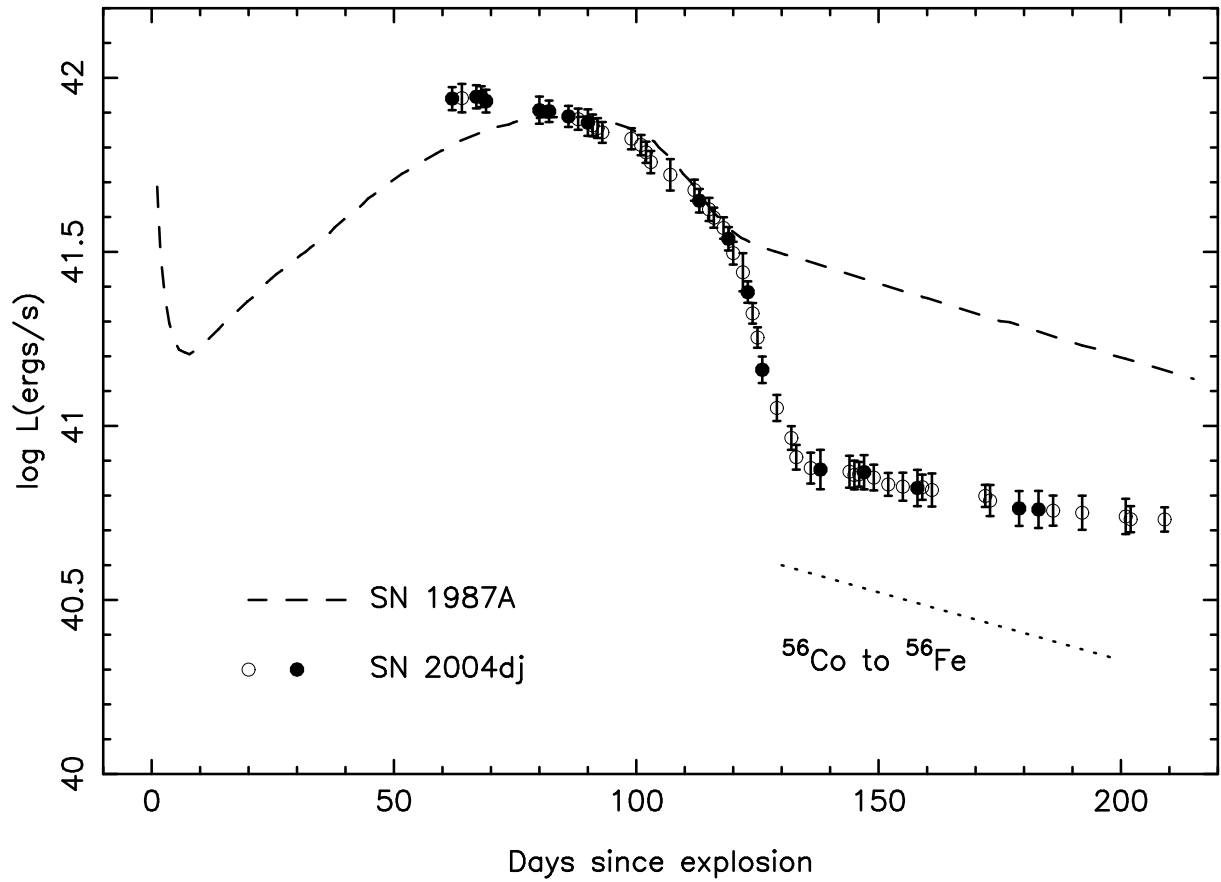


Fig. 8.— The bolometric light curve of SN 2004dj compared to that of SN 1987A. The open circles are interpolated data points. The reported errors are 1σ . The data of SN 1987A come from Suntzeff & Bouchet (1990). The dotted line is the slope of ^{56}Co to ^{56}Fe decay.

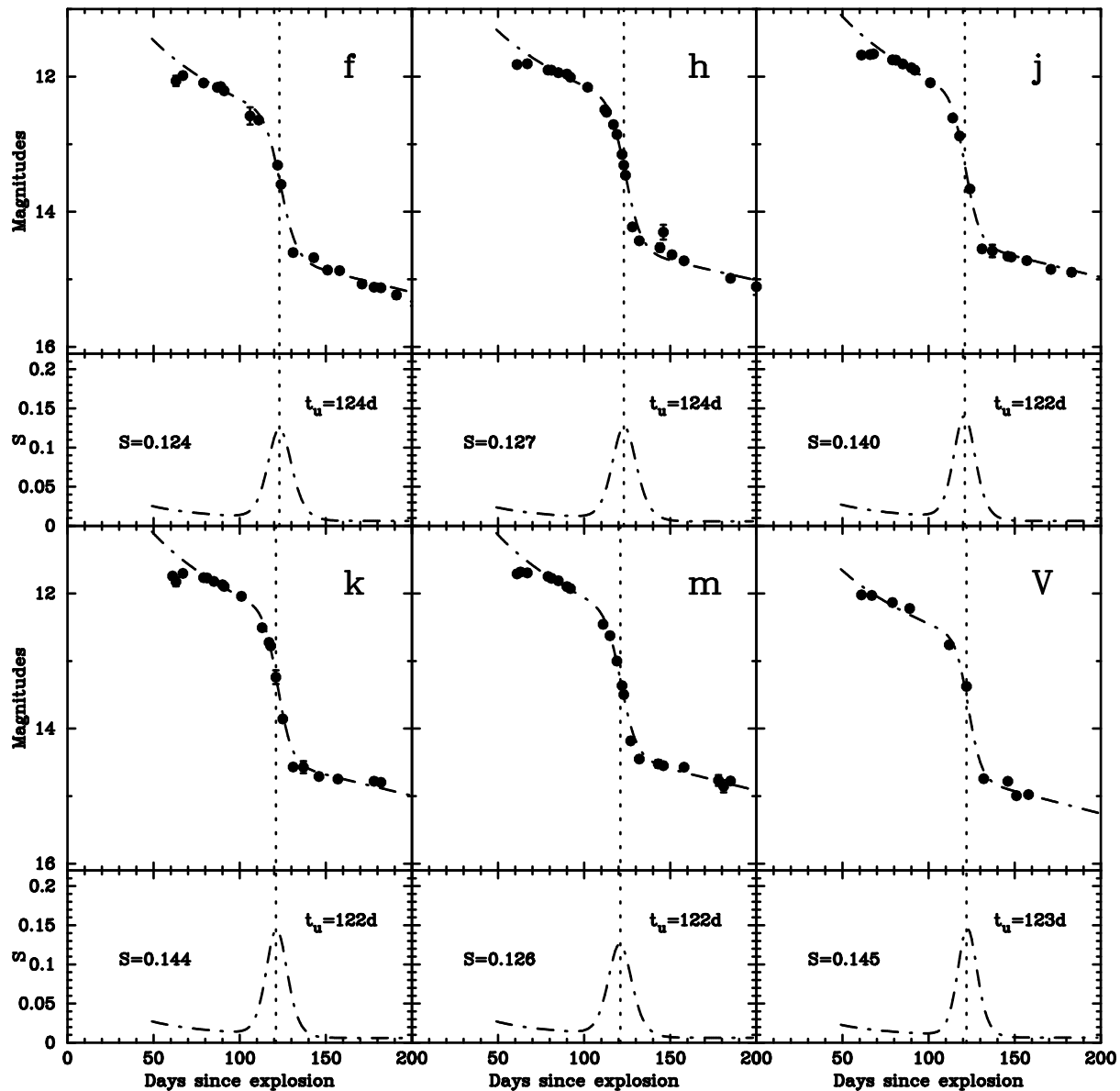


Fig. 9.— Determination of the steepness parameter and the time of inflection for the f , h , j , k , m , and V bands. For each passband, the upper panel shows the light curve (solid dots) together with the best fit (dashed curve), while the lower panel shows the profile for the steepness S parameter. The inflection time t_u is marked by a dotted line that corresponds to the maximum of S .

Table 1. Photometry of Comparison Stars

ID.	$\alpha(2000.0)$	$\delta(2000.0)$	d	e	f	g	h	i	j	k	m	n	o	p
1	07:35:09.74	65:46:36.5	13.30(01)	13.12(01)	12.94(01)	12.85(01)	12.78(01)	12.68(01)	12.57(01)	12.58(01)	12.55(01)	12.56(01)	12.52(01)	12.52(02)
2	07:35:10.62	65:44:02.4	14.22(01)	14.06(01)	13.90(01)	13.79(01)	13.73(01)	13.58(01)	13.50(01)	13.51(01)	13.45(01)	13.46(01)	13.39(03)	13.42(03)
3	07:37:21.71	65:42:41.4	13.06(01)	12.94(01)	12.81(01)	12.77(01)	12.74(01)	12.79(01)	12.55(01)	12.62(01)	12.58(01)	12.57(01)	12.58(02)	12.62(02)
4	07:38:02.01	65:42:03.3	14.06(01)	13.77(01)	13.57(01)	13.35(01)	13.25(01)	13.06(01)	12.92(01)	12.89(01)	12.84(01)	12.81(01)	12.75(02)	12.76(02)
5	07:35:14.21	65:34:13.1	14.12(01)	13.88(01)	13.72(01)	13.57(01)	13.52(01)	13.36(01)	13.22(01)	13.27(01)	13.23(01)	13.18(01)	13.20(02)	13.22(03)
6	07:39:15.32	65:33:11.9	13.91(01)	13.71(01)	13.54(01)	13.44(01)	13.39(01)	13.26(01)	13.16(01)	13.18(01)	13.14(01)	13.13(01)	13.11(02)	13.14(03)
7	07:36:12.57	65:31:41.2	13.72(01)	13.42(01)	13.22(01)	13.04(01)	12.95(01)	12.84(01)	12.66(01)	12.67(01)	12.60(01)	12.58(01)	12.52(01)	12.51(02)
8	07:36:48.80	65:30:53.3	13.23(01)	13.05(01)	12.93(01)	12.83(01)	12.79(01)	12.67(01)	12.56(01)	12.58(01)	12.53(01)	12.53(01)	12.50(01)	12.50(02)
9	07:36:50.58	65:24:06.2	13.96(01)	13.82(01)	13.69(01)	13.63(01)	13.61(01)	13.48(01)	13.37(01)	13.42(01)	13.37(01)	13.33(01)	13.34(02)	13.38(03)
10	07:37:13.64	65:53:08.3	13.59(01)	13.41(01)	13.25(01)	13.11(01)	13.05(01)	12.93(01)	12.79(01)	12.83(01)	12.79(01)	12.78(01)	12.73(02)	12.79(02)
11	07:34:36.72	65:57:59.6	13.36(01)	13.18(01)	13.00(01)	12.89(01)	12.81(01)	12.71(01)	12.58(01)	12.61(01)	12.56(01)	12.59(01)	12.55(01)	12.58(02)
12	07:39:37.89	65:49:20.6	14.21(01)	14.02(01)	13.90(01)	13.82(01)	13.75(01)	13.64(01)	13.49(02)	13.55(01)	13.52(01)	13.50(02)	13.51(03)	13.43(03)
13	07:39:25.03	65:44:04.4	13.57(01)	13.39(01)	13.21(01)	13.09(01)	13.03(01)	12.92(01)	12.77(01)	12.82(01)	12.78(01)	12.80(01)	12.72(02)	12.85(02)
14	07:40:58.95	65:32:20.1	12.66(01)	12.56(01)	12.41(01)	12.33(01)	12.31(01)	12.28(01)	12.10(01)	12.16(01)	12.10(01)	12.11(01)	12.11(01)	12.12(01)
15	07:34:13.90	65:44:54.6	13.07(01)	12.93(01)	12.82(01)	12.76(01)	12.72(01)	12.64(01)	12.54(01)	12.59(01)	12.56(01)	12.58(01)	12.57(01)	12.58(02)
16	07:33:52.97	65:31:28.5	13.76(01)	13.49(01)	13.28(01)	13.11(01)	13.05(01)	12.88(01)	12.74(01)	12.74(01)	12.67(01)	12.65(01)	12.60(01)	12.55(03)
17	07:34:37.01	65:31:55.4	12.32(01)	12.18(01)	12.04(01)	11.94(01)	11.91(01)	12.07(01)	11.68(01)	11.73(01)	11.70(01)	11.69(01)	11.68(01)	11.69(01)
18	07:38:30.15	65:15:59.4	13.36(01)	13.19(01)	13.04(01)	12.90(01)	12.85(01)	12.71(01)	12.60(01)	12.63(01)	12.55(01)	12.56(01)	12.57(02)	12.54(02)
19	07:41:13.26	65:24:06.0	12.63(01)	12.56(01)	12.44(01)	12.40(01)	12.38(01)	12.33(01)	12.20(01)	12.25(01)	12.22(01)	12.24(01)	12.26(01)	12.24(01)
20	07:39:12.62	65:25:01.3	13.98(01)	13.73(01)	13.57(01)	13.33(01)	13.24(01)	13.06(01)	12.92(01)	12.94(01)	12.85(01)	12.84(01)	12.83(02)	12.79(02)

Note. — All quantities are magnitudes. Uncertainties in the last two digits are indicated in parentheses. Uncertainties which are less than 0.01 indicate as 0.01 in the table.

Table 2. SN 2004dj photometric observations

Date(UT)	JD ^a	<i>d</i>	<i>e</i>	<i>f</i>	<i>g</i>	<i>h</i>	<i>i</i>	<i>j</i>	<i>k</i>	<i>m</i>	<i>n</i>	<i>o</i>	<i>p</i>	<i>V</i>	<i>R</i>	<i>I</i>
12/08/04	3230	12.35(01)	11.89(01)	11.82(01)	11.48(01)	11.68(01)	11.74(01)	11.71(01)	12.09(02)	11.69(02)	11.69(04)	12.00(05)	11.58(06)	11.67(06)
14/08/04	3232	...	12.12(02)	12.06(08)	11.42(04)	...	11.83(07)	11.68(03)	11.52(04)	...
17/08/04	3235	12.40(03)	12.08(01)	...	11.92(01)	11.67(01)	12.06(02)	...	11.60(04)
18/08/04	3236	11.98(01)	...	11.81(01)	11.48(01)	...	11.70(01)	11.70(01)	...	11.66(02)	...	12.04(06)	11.58(06)	11.66(07)
19/08/04	3237	12.42(02)	12.13(01)	...	11.93(01)	11.66(01)	12.07(02)	...	11.69(04)
30/08/04	3248	12.54(05)	12.20(03)	12.09(02)	12.03(02)	11.90(01)	11.60(01)	11.75(01)	11.77(01)	11.75(01)	12.11(02)	11.77(06)	11.77(05)	12.16(06)	11.71(05)	11.72(06)
01/09/04	3250	11.91(01)	11.58(01)	11.76(01)	11.77(01)	11.78(01)	12.09(02)	11.74(02)	...	12.17(06)	11.69(06)	11.70(07)
05/09/04	3254	...	12.24(01)	11.94(01)	11.65(01)	11.81(01)	11.82(01)	11.81(01)	12.12(01)	11.83(02)	11.75(06)	...
07/09/04	3256	12.66(01)	...	12.16(01)	12.08(01)	11.67(03)
09/09/04	3258	12.79(07)	12.30(03)	12.15(02)	12.11(02)	11.96(01)	11.70(01)	11.75(05)	12.23(05)	11.80(06)
10/09/04	3259	11.87(01)	11.87(01)	11.90(01)	12.16(02)	11.84(03)	11.80(07)
11/09/04	3260	...	12.29(01)	12.21(01)	11.90(01)	11.90(01)
12/09/04	3261	12.01(01)	...	11.90(01)	...	11.93(01)	12.13(01)	11.88(02)	11.72(07)
18/09/04	3267	12.25(01)	11.96(03)
20/09/04	3269	12.87(02)	11.85(01)	11.96(06)
21/09/04	3270	12.33(01)	12.09(01)	12.04(02)	...	12.18(01)	12.04(02)	...	12.46(08)	...	11.84(07)
22/09/04	3271	12.95(02)	12.16(01)	12.08(04)
26/09/04	3275	...	12.60(08)	12.58(13)	12.06(03)	12.16(06)	...
01/10/04	3280	...	12.78(02)	12.64(01)	...	12.49(01)	12.46(01)	...	12.40(02)
02/10/04	3281	13.33(03)	12.67(01)	12.53(01)	12.25(01)	...	12.51(01)	12.35(05)	12.78(06)	12.35(06)	11.96(08)
04/10/04	3283	12.61(02)	12.44(02)	...	12.49(05)
05/10/04	3284	...	12.90(01)	...	12.80(01)	...	12.33(01)	12.63(01)	12.92(06)	12.43(06)	12.21(10)
07/10/04	3286	13.50(03)	12.71(01)	12.73(02)
08/10/04	3287	...	13.04(02)	12.88(01)	12.78(01)	...	12.57(01)	12.73(02)	12.65(05)	12.37(06)
09/10/04	3288	13.03(03)	12.86(02)	12.55(01)	13.00(02)	12.61(07)	12.75(03)	...	13.15(06)	12.65(05)	12.32(10)
11/10/04	3290	...	13.35(02)	13.24(10)	...	12.61(07)	...	13.04(20)
12/10/04	3291	13.31(01)	13.28(01)	13.15(01)	12.86(01)	13.36(01)	...	13.08(03)	...	13.39(06)	12.96(05)	12.49(20)
13/10/04	3292	13.39(01)	13.31(01)	13.50(01)	12.93(02)
14/10/04	3293	13.60(01)	...	13.46(01)	...	13.66(02)
15/10/04	3294	14.43(04)	14.01(02)	13.31(01)	13.86(02)	...	13.12(02)	...	13.53(08)	...	13.41(05)	...
18/10/04	3297	14.36(03)	14.23(02)	14.18(03)	...	14.09(08)	...	14.47(06)	...	13.45(12)
21/10/04	3300	14.60(03)	14.55(04)	14.57(04)
22/10/04	3301	...	14.91(04)	...	14.66(04)	14.43(03)	14.45(04)	14.74(07)
25/10/04	3304	15.53(06)	14.04(03)	13.66(02)	14.30(07)	14.45(11)	14.86(10)	14.14(05)	13.43(07)
27/10/04	3306	15.46(14)	14.10(02)	14.58(10)	14.57(09)	14.20(07)	14.29(14)	...	14.21(02)	13.43(07)
02/11/04	3312	15.36(14)	...	14.68(05)	14.52(06)
03/11/04	3313	14.84(07)	14.53(10)	13.62(02)	14.95(13)
04/11/04	3314	...	15.43(04)	14.15(02)	14.45(06)
05/11/04	3315	15.69(10)	15.10(04)	...	14.59(04)	14.30(03)	14.10(02)	14.66(04)	14.71(04)	14.55(03)	13.63(02)	14.27(05)	14.19(12)	14.72(06)	14.20(05)	13.47(06)
07/11/04	3317	15.57(07)	15.13(03)	14.08(02)	14.67(04)	14.18(05)
10/11/04	3320	14.86(04)	14.87(03)	14.64(02)	14.99(07)
13/11/04	3323	14.11(01)	13.62(01)	14.29(07)	14.48(09)	15.00(06)	14.21(01)	13.37(12)
16/11/04	3326	15.81(09)	15.23(04)	14.72(04)	14.75(04)	...	13.58(02)	...	14.74(18)
17/11/04	3327	14.87(03)	14.88(04)	14.73(03)	14.57(03)	...	14.20(05)	...	14.98(06)	...	13.07(16)
19/11/04	3329	15.77(08)	15.13(04)	13.55(02)	...	14.56(15)
30/11/04	3340	15.07(03)	14.12(01)	14.85(03)	14.22(05)	...
01/12/04	3341	15.92(10)	15.27(07)	14.13(02)	14.41(09)	14.23(06)	...
07/12/04	3347	16.21(14)	...	15.12(03)	14.20(02)	...	14.78(04)	14.77(08)	...	14.58(10)	14.30(05)	...
11/12/04	3351	15.85(06)	...	15.13(03)	14.90(05)	14.80(04)	14.85(09)	13.57(02)	...	15.02(18)
14/12/04	3354	...	15.52(07)	...	15.11(05)	14.99(03)	14.78(04)	...	14.52(10)	...	15.22(06)	...	13.21(20)

Table 2—Continued

Date(UT)	JD ^a	<i>d</i>	<i>e</i>	<i>f</i>	<i>g</i>	<i>h</i>	<i>i</i>	<i>j</i>	<i>k</i>	<i>m</i>	<i>n</i>	<i>o</i>	<i>p</i>	<i>V</i>	<i>R</i>	<i>I</i>
20/12/04	3360	15.23(05)	14.11(01)	13.54(02)	...	14.90(18)	15.32(06)	14.21(06)	...
29/12/04	3369	...	15.50(08)	...	15.36(14)	15.11(12)	15.47(06)
30/12/04	3370	...	15.57(05)	15.36(03)	14.14(01)	14.71(07)	14.25(06)	...
06/01/05	3377	16.08(07)

^a2450000+

Table 3. The decline rates of different bands on the exponential phase.

Filter name	$\lambda(\text{\AA})$	Decline rate [mag (10 days) ⁻¹]
d	4540	0.10 ± 0.01
e	4925	0.08 ± 0.01
f	5270	0.11 ± 0.01
g	5795	0.11 ± 0.01
h	6075	0.11 ± 0.01
i	6656	0.00 ± 0.01
j	7057	0.07 ± 0.01
k	7546	0.06 ± 0.02
m	8023	0.07 ± 0.01
n	8480	-0.02 ± 0.01
o	9182	0.08 ± 0.01
p	9739	0.13 ± 0.03